

States in ^{121}Sn from the $^{120}\text{Sn}(d, p)^{121}\text{Sn}$ reaction at 17 MeV*

M. J. Bechara†

Instituto de Física, Universidade de São Paulo, São Paulo, Brasil

O. Dietzsch‡

*University of Pittsburgh, Pittsburgh, Pennsylvania,
and Instituto de Física, Universidade de São Paulo, São Paulo, Brasil*

(Received 10 February 1975)

The $^{120}\text{Sn}(d, p)^{121}\text{Sn}$ reaction has been investigated at a bombarding energy of 17 MeV. The proton groups were analyzed by a magnetic spectrograph and detected in nuclear emulsions with a resolution of ~ 10 keV. Excitation energies and angular distributions were obtained for levels below $E_x = 4.9$ MeV in ^{121}Sn . A distorted-wave analysis was used to determine l values and spectroscopic strengths. The results are compared to previous data from transfer reactions. Centers of gravity and sums of spectroscopic factors are presented for the detected levels and are compared with the results of pairing theory.

[NUCLEAR REACTIONS $^{120}\text{Sn}(d, p)$, $E = 17$ MeV, measured $\sigma(E_p, \theta)$. ^{121}Sn deduced level energies, l , j , π , spectroscopic strengths. Enriched targets.]

I. INTRODUCTION

Neutron transfer reactions on even Sn isotopes have been the subject of extensive studies over the past years.¹⁻⁶ Such studies have been complemented in recent years by the investigation of two-neutron transfer reactions,^{7,8} of Coulomb excitation,^{9,10} and of inelastic scattering.^{11,12} As a result, the main features of the level scheme of the odd isotopes of tin are now well understood¹³ and a good qualitative over-all agreement is found between the experimental data for low-lying levels and the results of theoretical calculations¹⁴⁻¹⁶ using the phenomenological pairing residual interaction as well as more realistic residual forces.

The ^{121}Sn nucleus is a good example of an odd tin isotope whose level structure has been thoroughly investigated with neutron transfer reactions. Schneid, Prakash, and Cohen² have studied the $^{120}\text{Sn}(d, p)^{121}\text{Sn}$ and the $^{122}\text{Sn}(d, t)^{121}\text{Sn}$ reactions; the $^{122}\text{Sn}(p, d)^{121}\text{Sn}$ reaction has been examined by Cavanagh *et al.*⁶; and Casten *et al.*⁷ reported measurements on the $^{120}\text{Sn}(t, d)^{121}\text{Sn}$ and the $^{119}\text{Sn}(t, p)^{121}\text{Sn}$ reactions. While reasonable agreement is found among the results of these works concerning the strong transitions, a number of serious discrepancies also exist.

The present study attempts to confirm and elucidate spin and level assignments in ^{121}Sn . It presents the results of the $^{120}\text{Sn}(d, p)^{121}\text{Sn}$ reaction at a bombarding energy of 17 MeV investigated with a resolution of ~ 10 keV. Long exposures were also made in an attempt to detect states with small cross sections. These features resulted in the

discovery of many new energy levels and for many of them quantum numbers could be assigned. This paper is part of a series of high-resolution (d, p) and (d, t) reaction studies in the tin isotopes. Previous publications¹⁷⁻¹⁹ have dealt with the level structure of ^{111}Sn , ^{113}Sn , ^{119}Sn , and ^{123}Sn , and subsequent papers will report on reactions on other stable isotopes of tin.

II. EXPERIMENTAL PROCEDURE

Targets enriched to 98.39% in ^{120}Sn were bombarded by 17 MeV deuterons from the three-stage Van de Graaff accelerator of the University of Pittsburgh. Details of the beam transport system have been described previously.^{20, 21} The targets consisted of deposits (about $70 \mu\text{g}/\text{cm}^2$ thick) of the metal evaporated over a small rectangular area, about 0.5 mm wide and 3.0 mm high centered on a thin carbon backing ($20 \mu\text{g}/\text{cm}^2$). With such targets, narrow beam-defining slits in front of the target do not have to be employed, with the advantage of elimination of slit-edge scattering. The scattered protons were analyzed in an Enge split-pole magnetic spectrograph²² and detected in nuclear emulsion plates (Kodak NTB, $25 \mu\text{m}$ thick) placed in the focal surface of the spectrograph. The emulsions were covered with aluminum foils of enough thickness to absorb heavier reaction products. The elastically scattered deuterons were continuously monitored by two NaI(Tl) scintillators symmetrically located at $\pm 38^\circ$ with respect to the incident beam direction. The exposed plates were later scanned at the University of

São Paulo at 0.2 mm intervals along the plate.

Proton spectra were obtained at 14 angles from 8° to 60° . The spectrum observed at a laboratory scattering angle of 24° is shown in Fig. 1. The proton groups from the excited states of ^{121}Sn are numbered, the ground state group being labeled zero. The energy resolution in this spectrum, of the order of 10 keV full width at half-maximum can be regarded as typical of the spectra obtained at other angles. In Fig. 1, peaks which are not numbered were identified as groups arising from (d,p) reactions on nuclei other than ^{120}Sn . Groups from reactions on very light impurities could easily be detected by their larger widths and their greater energy variation with the scattering angle. Groups from other isotopes of tin which were present in the target were identified from a comparison with spectra obtained at two different scattering angles with a target made from a blended tin metal which contained approximately equal amounts of all even tin isotopes.¹⁷ In the identification of weakly excited levels the fact was exploited that the relative distances of peaks due to energy levels in tin isotopes are the same (within 0.4 mm) at all angles. The spectra obtained at different angles were summed point by point after making the respective ground states coincide. In the resulting sum spectrum, peaks of tin isotopes are reinforced while random background and contaminant peaks due to lighter or heavier nuclei are not. However, we cannot rule out entirely the presence of peaks due to contaminant nuclei of

mass similar to tin.

The excitation energies tabulated in Table I represent the average of the excitation energies computed at each angle making use of the calibration of the focal plane.²³ The rms deviation of energy measurements at 14 angles was typically 2 keV. The absolute excitation energy scale is uncertain by $\pm 0.25\%$.

Relative normalization of the (d,p) cross sections was obtained from the pair of NaI(Tl) counters detecting the elastically scattered deuterons. The absolute normalization of reaction cross sections was obtained from the knowledge of the 17 MeV deuteron elastic cross section at the monitor angle (38° in our case) given by an optical model prediction using the parameters shown in Table II. It is estimated that the absolute values for the cross sections have an uncertainty of $\pm 25\%$.

Angular distributions were extracted for 40 levels up to 4.83 MeV excitation energy. They are shown in Figs. 2-5.

III. DISTORTED-WAVE BORN APPROXIMATION ANALYSIS

The angular distributions were compared with the predictions of zero-range distorted-wave calculations using the code JULIE.²⁴ The optical model parameters for the entrance and exit channels were taken from Perey's analysis^{25, 26} of deuteron and proton scattering. These parameters are listed in Table II. The captured neutron was

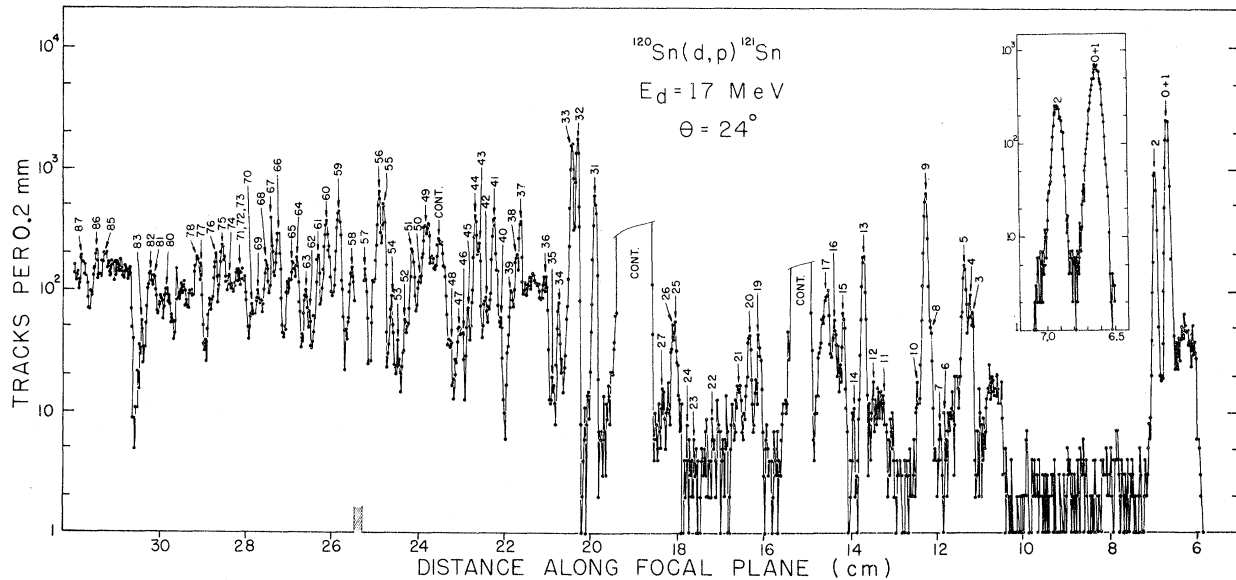


FIG. 1. The proton spectrum from the $^{120}\text{Sn}(d,p)^{121}\text{Sn}$ reaction at $\theta_{\text{lab}} = 24^\circ$. The proton groups are labeled with the numbers used to identify the corresponding ^{121}Sn levels in Table I. The insert shows the ground state region scanned with higher magnification and in smaller steps.

TABLE I. Summary of the results for ^{121}Sn from the $^{120}\text{Sn}(d,p)^{121}\text{Sn}$ reaction and a comparison with previous experiment.

Level Number	E_x (MeV)	Results of the present experiment $E_d = 17$ MeV (d, p)				Schneid <i>et al.</i> (Ref. 2) $E_d = 15$ MeV (d, p)				
		l	j^π	$\left(\frac{d\sigma}{d\Omega}\right)_{\text{max}}$ (mb/sr)	S_{lj}	E_x (MeV)	l	j^π	$\left(\frac{d\sigma}{d\Omega}\right)_{\text{max}}$ (mb/sr)	S_{jl}
0 ^a	0.0	(2)	$(\frac{3}{2}^+)$	(3.696)	0.439	0.0	2	$\frac{3}{2}^+$	3.17	0.43
(1)	...	(5)	$(\frac{11}{2}^-)$	(0.864)	0.488					
2	0.058	0	$(\frac{1}{2}^+)$	1.303	0.302	0.05	0	$\frac{1}{2}^+$	1.93	0.39
3 ^a	0.899	(2)	$(\frac{5}{2}^+)$	(0.225)	0.014					
4	0.916	(4)	$(\frac{7}{2}^+)$	(0.100)	0.033	0.93	4	$\frac{7}{2}^+$	0.276	0.19
5	0.941	3	$(\frac{7}{2}^-)$	0.264	0.024					
6	1.022			0.03 ^b						
7	1.058			0.02 ^b						
8	1.089			0.10 ^c						
9	1.113	2	$(\frac{5}{2}^+)$	1.174	0.075	1.12	2	$\frac{5}{2}^+$	1.03	0.065
10	1.147			0.03 ^b						
11	1.328			0.01 ^b						
12	1.355	(4)	$(\frac{7}{2}^+)$	0.014	0.004					
13	1.395	2	$(\frac{5}{2}^+)$	0.416	0.023	1.40	2	$\frac{5}{2}^+$	0.477	0.029
14	1.441			0.15 ^d						
15	1.489			0.13 ^d						
16	1.528			0.07 ^d						
17	1.562			0.03 ^b						
18	1.700	2	$(\frac{5}{2}^+)$	0.110	0.006	1.71	2	$(\frac{5}{2}^+)$	0.082	0.004
19	1.857	1	$(\frac{3}{2}^-)$	0.157	0.007					
20	1.901	1	$(\frac{3}{2}^-)$	0.131	0.006	1.91	(1)	$(\frac{3}{2}^-)$	0.125	0.007
21	1.950	(1)	$(\frac{3}{2}^-)$	0.039	0.002					
22	2.066			0.019 ^b		2.06	(3)	$(\frac{7}{2}^-)$	0.047	0.005
23	2.156			0.02 ^d						
24	2.181			0.01 ^d						
25	2.233			0.06 ^d						
26	2.247			0.07 ^d		2.25	(2)	$(\frac{5}{2}^+)$	0.503	0.027
27	2.289			0.03 ^d						
28	2.361			0.05 ^d						
29	2.424			0.03 ^e						
30	2.451			0.110 ^e		2.45	(3)	$(\frac{7}{2}^-)$	0.234	0.021
31	2.578	3	$(\frac{7}{2}^-)$	0.864	0.045	2.59	(3)	$(\frac{7}{2}^-)$	0.405	0.035
32	2.660	3	$(\frac{7}{2}^-)$	1.436	0.079	2.69	(3)	$(\frac{7}{2}^-)$	2.24	0.185
33	2.682	3	$(\frac{7}{2}^-)$	1.880	0.092					
34	2.739			0.09 ^d						
35	2.768			0.02 ^d						
36	2.799			0.20 ^d						
37	2.906	(3)	$(\frac{7}{2}^-)$	0.429	0.023	2.93			0.432	
38	2.921			0.25 ^c						
39	2.946			0.20 ^c						
40	2.990			0.10 ^c						

TABLE I (Continued)

Level Number	E_x (MeV)	Results of the present experiment $E_d=17$ MeV (d, p)				Schneid <i>et al.</i> (Ref. 2) $E_d=15$ MeV (d, p)				
		l	j^π	$\left(\frac{d\sigma}{d\Omega}\right)_{\text{max}}$ (mb/sr)	S_{ij}	E_x (MeV)	l	j^π	$\left(\frac{d\sigma}{d\Omega}\right)_{\text{max}}$ (mb/sr)	S_{ji}
41	3.019	(3, 1)	$(\frac{1}{2}^-, \frac{3}{2}^-)$	0.928	(0.041, 0.053)	3.10	(1)	$(\frac{3}{2}^-)$	2.01	0.13
42	3.060			0.15 ^c						
43	3.087			0.50 ^d						
44	3.098			0.50 ^d						
45	3.136			0.09 ^d						
46	3.159			0.05 ^d						
47	3.176			0.05 ^d						
48	3.214			0.03 ^d						
49 ^f	3.312	(1)	$(\frac{3}{2}^-)$	0.567	0.031					
50	3.341			0.10 ^c						
51	3.369			0.656 ^g		3.37	(1)	$(\frac{3}{2}^-)$	1.32	0.077
52	3.390			0.30 ^c						
53	3.425	(0)	$(\frac{1}{2}^+)$	0.089	0.014					
54	3.450			0.247 ^g						
55	3.490	(3, 4)	$(\frac{1}{2}^-, \frac{7}{2}^+)$	0.656	(0.024, 0.110)					
56	3.506	(1)	$(\frac{3}{2}^-)$	1.683	0.086	3.51	(1)	$(\frac{3}{2}^-)$	2.44	0.15
57	3.570			0.479 ^g						
58	3.611	(3)	$(\frac{1}{2}^-)$	0.321	0.013					
59	3.667	1	$(\frac{3}{2}^-)$	1.168	0.059	3.69	(1)	$(\frac{3}{2}^-)$	2.44	0.14
60	3.721	1	$(\frac{3}{2}^-)$	1.179	0.059					
61	3.757	1	$(\frac{3}{2}^-)$	0.447	0.023					
62 ^a	3.789	1	$(\frac{3}{2}^-)$	(0.079)	0.004					
63	3.805	1	$(\frac{3}{2}^-)$	(0.227)	0.011					
64	3.848	1	$(\frac{3}{2}^-)$	0.488	0.024					
65	3.866	1	$(\frac{3}{2}^-)$	0.582	0.027	3.85	(1)	$(\frac{3}{2}^-)$	0.600	0.037
66	3.926	1	$(\frac{3}{2}^-)$	0.862	0.044					
67	3.951	1	$(\frac{3}{2}^-)$	0.410	0.022	3.93	(1)	$(\frac{3}{2}^-)$	1.53	0.095
68	3.975	1	$(\frac{3}{2}^-)$	0.513	0.025					
69	4.011			0.40 ^c						
70	4.037			0.30 ^c						
71	4.064			0.40 ^c						
72	4.085			0.40 ^c						
73	4.102			0.30 ^c						
74	4.135			0.20 ^c						
75	4.162	1	$(\frac{3}{2}^-)$	1.110	0.044	4.16	(1)	$(\frac{3}{2}^-)$	1.14	0.073
76	4.190			0.893 ^g						
77 ^a	4.255			1.180 ^g		4.25	(1)	$(\frac{3}{2}^-)$	0.830	0.053
78	4.268									
79	4.321			1.00 ^c						
80	4.392			0.291 ^g						
81	4.444			0.30 ^c						
82	4.459			0.30 ^c						

TABLE I (Continued)

Level Number	Results of the present experiment $E_d = 17$ MeV (d, p)					Schneid <i>et al.</i> (Ref. 2) $E_d = 15$ MeV (d, p)				
	E_x (MeV)	l	j^π	$\left(\frac{d\sigma}{d\Omega}\right)_{\max}$ (mb/sr)	S_{lj}	E_x (MeV)	l	j^π	$\left(\frac{d\sigma}{d\Omega}\right)_{\max}$ (mb/sr)	S_{lj}
83	4.489			0.20 ^c						
84	4.530			0.40 ^c						
85	4.646			0.70 ^c						
86	4.680	(1)	$\left(\frac{3}{2}^-\right)$	0.434	0.029					
87	4.736	(3, 4)	$\left(\frac{7}{2}^-, \frac{7}{2}^+\right)$	0.558	(0.018, 0.070)					
88	4.773			0.40 ^c						
89	4.826	(3, 4)	$\left(\frac{7}{2}^-, \frac{7}{2}^+\right)$	0.508	(0.017, 0.070)					
90	4.905			0.70 ^c						

^a This level and the next one are members of an unresolved doublet.

^b A meaningful comparison of the angular distribution to DWBA curves was not possible due to the poor statistics of the data.

^c This level was not completely resolved from neighboring peaks; only a rough estimate for its cross section is given.

^d Cross sections were not determined for angles below 20° due to the presence of a strong peak of a light contaminant.

^e Cross sections were not determined for angles between 20° and 36° due to the presence of a strong peak of a light contaminant.

^f The experimental evidence suggests that this level may be an unresolved doublet.

^g Angular distribution does not show a stripping pattern.

assumed to be bound by a conventional Woods-Saxon potential well defined by $r_0 = 1.25$ fm, $a = 0.65$ fm, and $\lambda_{so} = 25$. The well depth is adjusted by the code to reproduce the appropriate binding energy. A lower cutoff radius of 6.2 fm in the radial integrals was employed in these calculations. Distorted-wave Born approximation (DWBA) calculations were also made with the code DWUCK²⁷ using both the nonlocal and finite-range corrections available in the code. The correction parameters employed were $\beta_d = 0.54$ fm, $\beta_p = 0.85$ fm, and $R = 0.62$ fm. It was found that these corrections lead to spectroscopic factors which differ by less than 10% from those obtained from the zero-range calculations employing a lower cutoff radius while there are negligible differences in the angular distribution shapes at the forward angles.

The fits to the angular distributions are also shown in Figs. 2–5 in comparison with the data whenever an assignment of the value of the transferred angular momentum was attempted. The fitting procedure adopted here involved matching the DWBA reaction cross section to the average shape of the experimental angular distribution around the position of the first forward-angle maximum. The over-all quality of the fits is reasonably good except for $l = 1$ transitions where a few states could not be fitted at angles above the

first maximum. No attempts were made, however, to improve the situation through a variation of potential parameters. The spectroscopic factors listed in column 6 of Table I were computed in the usual way²⁴ employing the relationship

$$\left(\frac{d\sigma}{d\Omega}\right)_{\text{exp}} = 1.48(2j+1)S_{lj}\sigma_{\text{DW3A}},$$

where l and j are the orbital and total angular momenta of the transferred neutron, respectively, and S_{lj} is the associated spectroscopic factor.

The adopted j values reproduced in column 4 of Table I are those predicted by the shell model.

TABLE II. Bound-state and optical model parameters used in DWBA calculations.

	Deuteron	Bound Neutron	Proton
r_c (fm)	1.15		1.25
V (MeV)	97.4	a	53.0
r_0 (fm)	1.15	1.25	1.25
a (fm)	0.81	0.65	0.65
W (MeV)	0		0
W' (MeV)	18.5		13.5
r'_0 (fm)	1.34		1.25
a' (fm)	0.68		0.47
V_{so} (MeV)	0	$\lambda_{so} = 25$	7.5

^a Adjusted to reproduce the neutron binding energy.

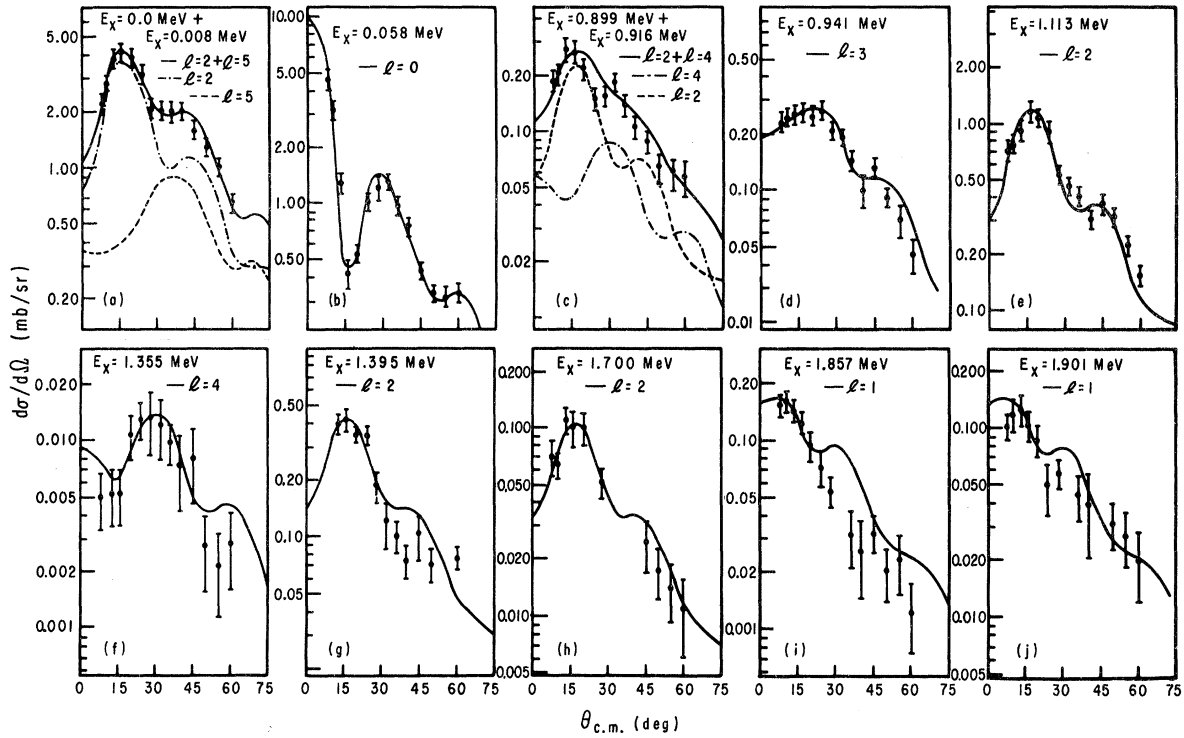


FIG. 2. Angular distributions of transitions in the $^{120}\text{Sn}(d, p)^{121}\text{Sn}$ reaction. The experimental points are given with error bars corresponding to statistics and background subtraction. The solid lines are DWBA curves fitted to the experimental data.

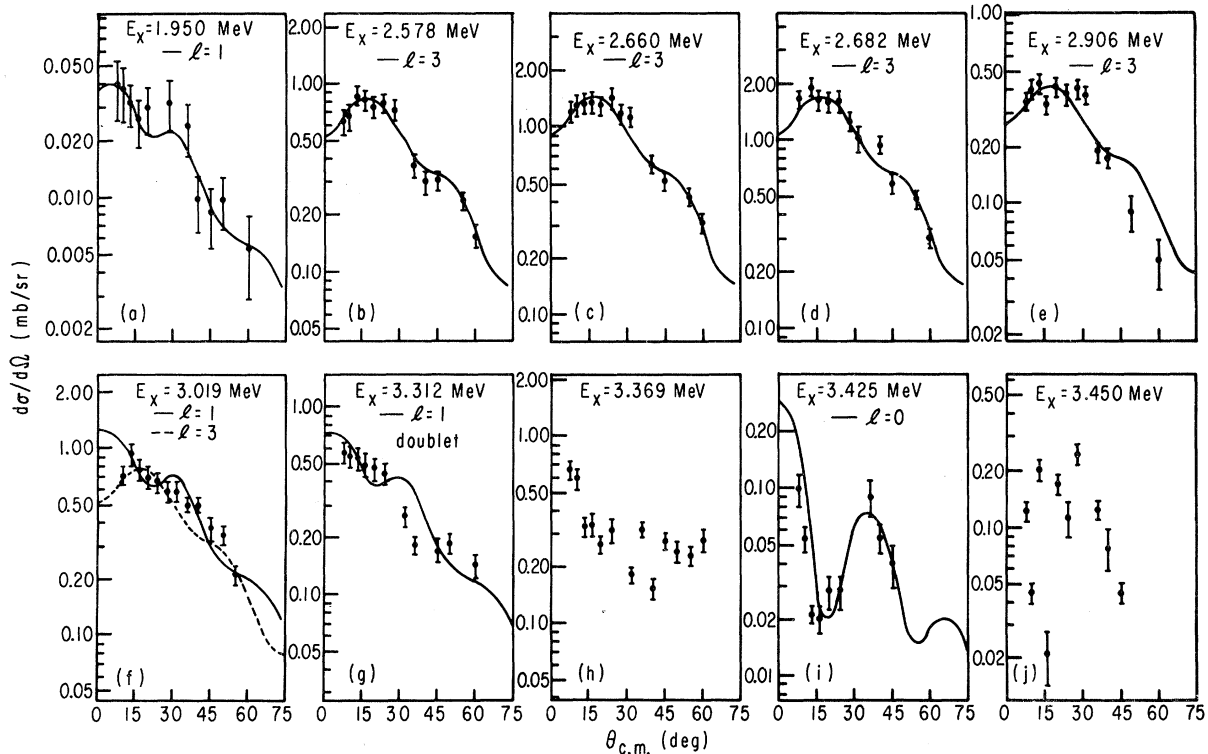
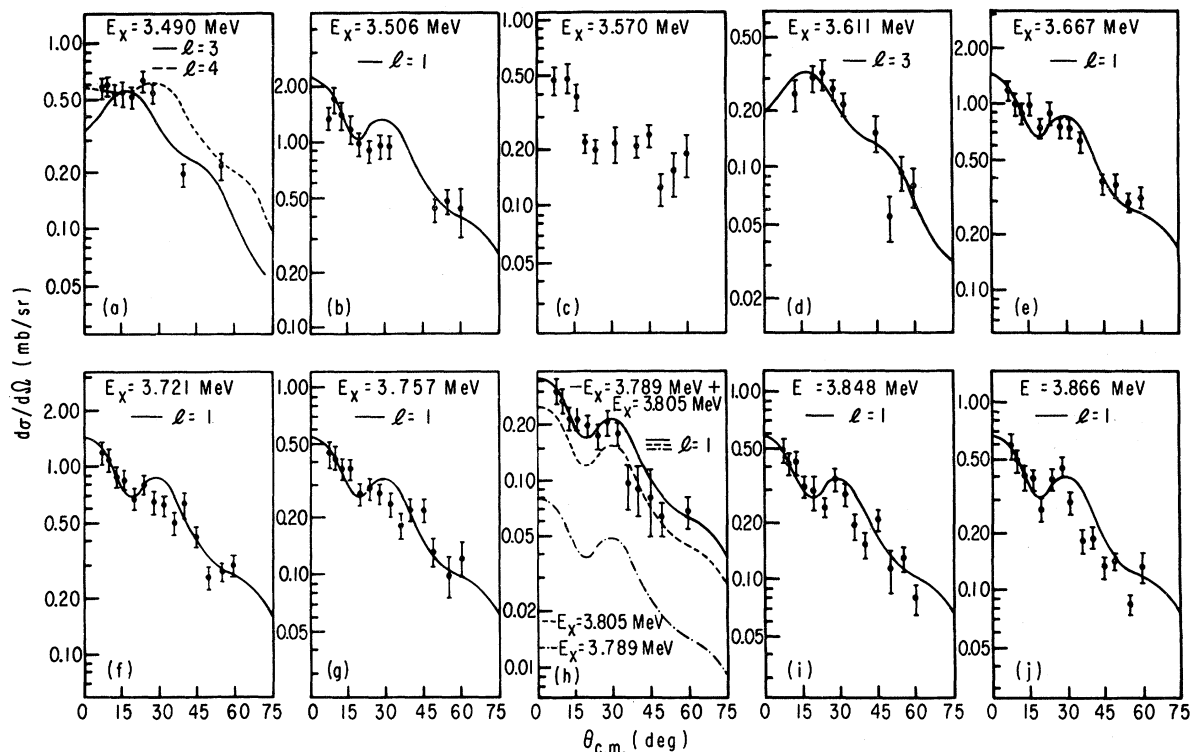
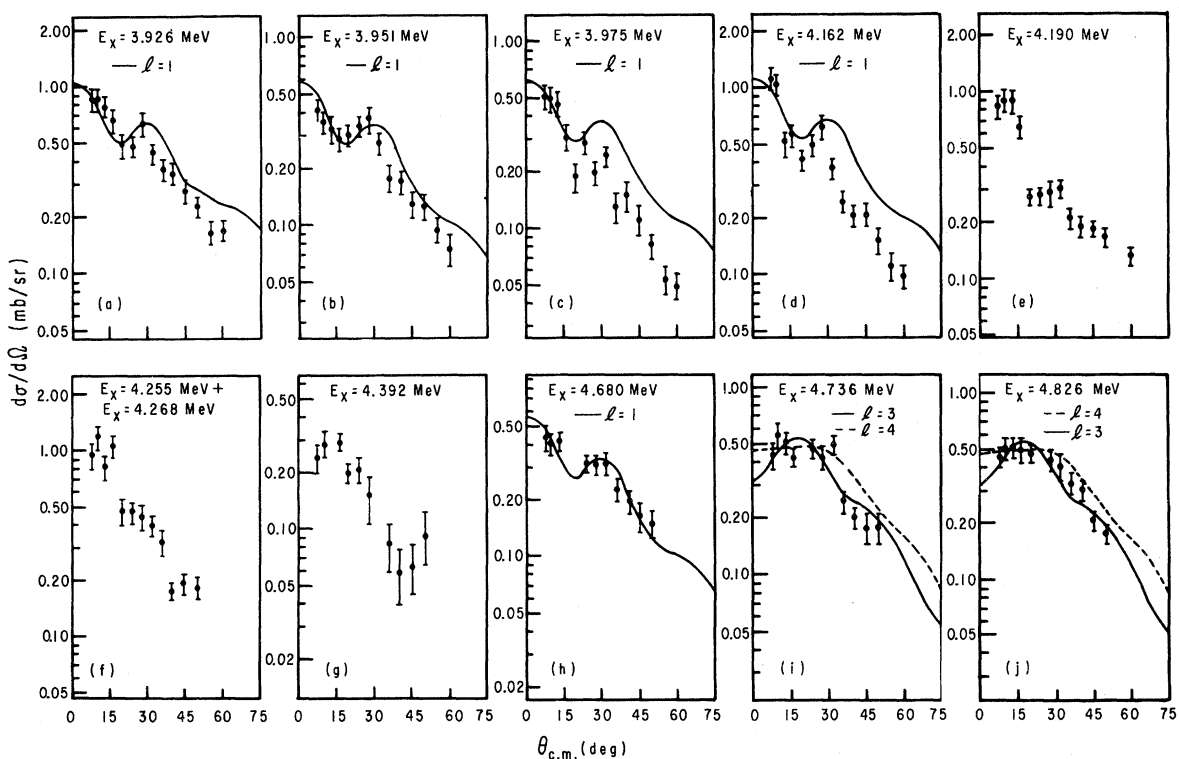


FIG. 3. The $^{120}\text{Sn}(d, p)$ angular distributions (continued).

FIG. 4. The $^{120}\text{Sn}(d,p)$ angular distributions (continued).FIG. 5. The $^{120}\text{Sn}(d,p)$ angular distributions (continued).

For the 50–82 neutron shell the orbits being filled are $2d_{3/2}$, $1h_{11/2}$, $3s_{1/2}$, $2d_{5/2}$, and $1g_{7/2}$. The ambiguity for the $l=2$ transitions could be resolved in cases for which there exist spectroscopic information on the $(d,t)^2$ or $(p,d)^6$ reactions. Use was made of the fact that the ratio of spectroscopic factors for a neutron capture and a neutron pickup transition to the same state is the same for all final states of same spin and parity^{1,28} and is proportional to U_j^2/V_j^2 . The ratio should be larger for a $d_{3/2}$ state than for a $d_{5/2}$ state since the latter lies lower than the former and therefore should be fuller. Levels corresponding to transitions with $l=1$ and $l=3$ were assigned $j^\pi = \frac{3}{2}^-$ and $\frac{7}{2}^-$, respectively, since they correspond to the lower energy levels in the 82–126 neutron shell.

IV. RESULTS AND DISCUSSION

A. Energy level spectrum

The results for the excitation energies, experimental cross sections, orbital angular momenta, and spectroscopic strengths are summarized in Table I. There we also list the results of Schneid *et al.*² for the $^{120}\text{Sn}(d,p)^{121}\text{Sn}$ reaction at $E_d = 15$ MeV. A comparison reveals that many levels seen in the previous (d,p) work² are now resolved in multiplets of close-lying states. Also a great number of weak states were detected in the present experiment which had not been observed before.

The level scheme of ^{121}Sn has been discussed already in considerable detail in the work of Casten *et al.*⁷ We review briefly here the new experimental information stressing the points where a discrepancy exists with previous works. The ground state is known²⁹ to have $j^\pi = \frac{3}{2}^+$. The angular distribution for the ground state peak reveals however very clearly [see Fig. 2(a)] an admixture of two l values (2 and 5). An $h_{11/2}$ state must then be present at an excitation energy of less than 10 keV since we were not able to resolve it from the ground state (see insert in Fig. 1) within the 10 keV resolution of the present experiment. This corroborates the findings of Snyder and Beard³⁰ for the β decay of $^{121}\text{Sn}^m$ (50 y) where an excitation energy of 8 ± 5 keV is attributed to this state. Cavanagh *et al.*⁶ and Schneid *et al.*² had already proposed the presence of this level near the ground state from considerations based on the systematics of the other tin isotopes, but they did not observe it in their low-resolution experiments. Casten *et al.*⁷ also did not detect any l admixture for the ground state transition in their high-resolution study of the (t,d) and (t,p) reactions. Our result leaves no doubt, however, as to the presence of the $h_{11/2}$ state near the ground state. The spectroscopic strengths for the $d_{3/2}$ ground state and the

$s_{1/2}$ 58 keV level are in good agreement with the previous (d,p) work but differ by as much as 50% from the results of the (t,d) reaction.

Near 900 keV we observe a triplet of states while the data of Casten *et al.*⁷ show a total of four levels. The previous (d,p) work² revealed only one state at 930 keV with $l=4$ and the (p,d) work⁶ detected one group at $E_x = 934$ keV which showed an admixture of d and g strengths. The lowest member of the multiplet observed by Casten *et al.*⁷ was excited only in the (t,p) reaction and was not detected in any of the one-nucleon transfer reaction experiments, ours included. It is thus a good candidate for having mostly a three-quasiparticle nature. The two lower states of our triplet could not be completely resolved at all angles. The angular distribution of the two groups combined [see Fig. 2(c)] shows that $l=2$ and $l=4$ are contributing to the reaction cross section. The relative strength of these two components that fits best our angular distribution is in considerable disagreement with the result reported by Casten *et al.*⁷ We were not able to fit our data using the ratio of strengths predicted by their data. The $l=2$ level (899 keV) can be either a $d_{3/2}$ or a $d_{5/2}$ state; it is tentatively given a $(\frac{5}{2}^+)$ assignment. The last member of this multiplet ($E_x = 0.941$ MeV) which appears as an $l=0$ state in the (t,d) experiment⁷ shows up in our data with a very clear $l=3$ angular distribution [see Fig. 2(d)]. Low-lying $f_{7/2}$ states near 1 MeV in excitation are now known to exist in many of the odd tin isotopes.^{19,5}

Only for the stronger member ($E_x = 1113$ keV) of the triplet near 1100 keV could we get a complete angular distribution. This is probably the state excited in the (p,d) reaction⁶ and which was also observed in the previous (d,p) work.² It corresponds to the higher member of the doublet observed in the (t,d) and (t,p) reaction.⁷ There is complete agreement among all these works as to the assignment of $j^\pi = \frac{5}{2}^+$ to this state. The lower member of our triplet at $E_x = 1089$ keV is probably the $l=2$ state observed by Casten *et al.*⁷ as the lower member of their doublet. While the 1113 keV level carries the major part of the $d_{5/2}$ quasiparticle strength, smaller amounts are located in states at 1395 and 1700 keV. The splitting of the $d_{5/2}$ strength is a systematic feature in tin nuclei and has been observed before not only in transfer reactions but also in elastic scattering of protons through isobaric analog states.³¹ The analogs of the states at 1113 and 1395 keV have been also observed in the scattering of a polarized proton beam and the measured polarization³² through the resonances are well fitted with $j^\pi = \frac{5}{2}^+$ for both states.

We located also a second $l=4$ state at $E_x = 1355$ keV which presumably contains a small fraction

of the $g_{7/2}$ strength. This state has not been observed before in transfer reactions. Seven other levels were detected between 1.0 and 1.7 MeV which also have not been reported before; but being weak or mixed with contaminants they could not have their angular momenta determined.

A triplet of $l=1$ states has been detected near 1900 keV of which only the central level had been identified previously by Schneid *et al.*² as being a p state. It is probably the level at 1.93 MeV seen in the (p, d) reaction as $l=2$. It was also excited in (t, p) and (t, d) but no l value was quoted.⁷ The higher member of the triplet might correspond to the 1.98 MeV $l=0$ level seen in (p, d) or to the 1953/1968 keV $l=0$ state seen in the $(t, d)/(t, p)$ reaction. But since both our angular distribution for this state (1901 keV) and the angular distribution for the 1968 keV state observed in (t, p) leave no doubt as to the respective l assignment, we must conclude that we are dealing with two different states. This is consistent with the interpretation advanced by Casten *et al.*⁷ that their states at 1968 keV ($L=0$) and 1876 keV ($L=5$) (which we also did not detect) are mostly of a three-quasiparticle nature. It is surprising, however to find some p strength at such low energies since we expect its centroid to lie at energies close to 4 MeV. Low-lying $l=1$ weak states have also been observed¹⁷ in ^{113}Sn and ^{123}Sn near 2.2 MeV but not in ^{119}Sn .¹⁸

From 2.0 to 2.5 MeV a large number of levels exists, some of them (e.g. peaks Nos. 25 and 26) with appreciable cross sections, but unfortunately no conclusive information about the l values could be extracted from the angular distributions because of the presence of light contaminants in spectra taken at angles below 20° . Several levels were also observed in previous works in this region but with no apparent correlation between data of different workers. Most of the states that were observed only in the (t, p) reaction from 2290 to 2513 keV are claimed by Casten *et al.*⁷ to be of a three-quasiparticle nature. It would be of interest to investigate the correlation with one-nucleon transfer data.

Above 2.5 MeV the level density starts to get too high and it was possible to identify only the stronger states. The high level density prevented also a detailed comparison to the other data. Three states (Nos. 31, 32, and 33) are very prominent and stand out strongly in this region. Together they carry more than 50% of the $f_{7/2}$ single-particle strength detected in this experiment. The presence of $f_{7/2}$ states at energies as low as 2.5 MeV is also a systematic feature in tin nuclei. The argument that the core-particle coupling [mainly $3^- (\times) s_{1/2}$ and $3^- (\times) d_{3/2}$] is responsible

for the splitting of the $f_{7/2}$ strength is confirmed by the strong transitions to the collective 2^+ and 3^- states in the even nuclei observed in the decay of the isobaric analog resonances corresponding to these states.^{33, 34}

The great majority of levels between 3.0 and 4.8 MeV for which a complete angular distribution could be determined are of an $l=1$ character. The heavy fragmentation of the p strength is evident in Fig. 6. Most of the states detected in this energy region in previous works are shown here to consist of more complicated structures. Two unresolved doublets (Nos. 49 and 62/63) present angular distributions [see Figs. 3(g) and 4(h)] which are well fitted by $l=1$ curves. The decomposition of strengths for levels Nos. 62 and 63 is somewhat arbitrary and there is more uncertainty in the results for this case. States Nos. 41, 55, 87, and 89 could be fitted by more than one value [see Figs. 3(f), 4(a), 5(i), and 5(j)]. An $l=3$ assignment is tentatively made for those states.

It is quite obvious from the preceding discussion that there are considerable discrepancies between the excitation energies quoted by the several authors for those strong states which could be un-

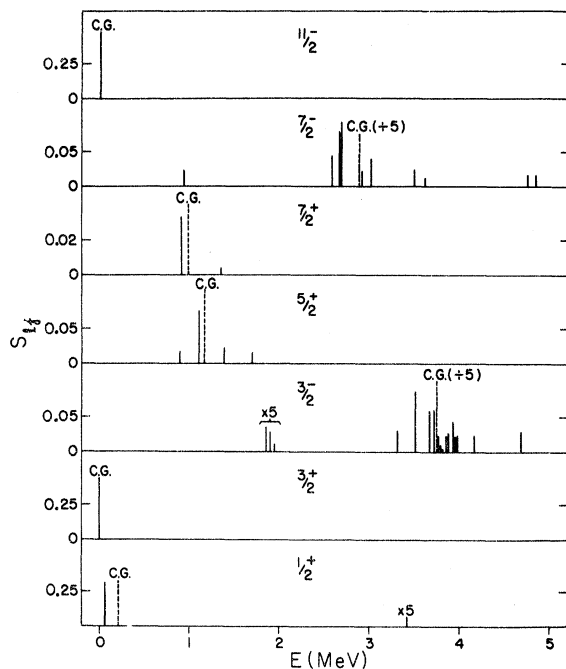


FIG. 6. Fragmentation of single-particle strengths among levels belonging to the same shell-model state in ^{121}Sn . The height of each line is proportional to the spectroscopic factor for each level. The heights of the dashed lines at the energies of the centers of gravity E'_{lj} are proportional to the sum of spectroscopic factors for states of same lj .

ambiguously identified in all works. Our energies are systematically lower by 10 keV than those quoted by Schneid *et al.*² and by Casten *et al.*⁷ from the (t, d) reaction. The energies quoted by Casten *et al.*⁷ from the (t, p) reaction are higher than ours by 10 to 30 keV. Differences up to 40 keV exist between our energies and those quoted by Cavanagh *et al.*⁸

B. Core-particle coupled states

The distribution of spectroscopic strength as a function of excitation energy for each subshell is shown in Fig. 6 where the heights of the lines are proportional to the spectroscopic factors. The low-lying (single-particle) levels show very little fractioning and are thus reasonably pure single-quasiparticle states. The spreading of the strength among several levels for the higher subshells indicates that these states have a more complicated structure. The most likely mechanism causing this spreading among low excited levels seems to be the core-particle coupling. There is a good indication⁷ that the positive-parity levels below 1.5 MeV result from admixtures of quasiparticle states ($d_{3/2}$, $s_{1/2}$, $d_{5/2}$, $g_{7/2}$) and states that result from the coupling of the $d_{3/2}$ and $s_{1/2}$ low-lying quasiparticles to the first 2^+ state in ^{120}Sn at 1.1 MeV.

The negative-parity states which have been identified at low excitations for the first time in the present experiment seem also to be amenable to an interpretation along the lines of the core-coupling model. The $l=3$ level at $E_x=941$ keV can be accounted for on the basis of the coupling of the $2f_{7/2}$ single-particle level to an $h_{11/2}$ particle plus 2^+ phonon mode. Calculations^{19, 35} taking into account such coupling have reproduced the magnitude of the absolute spectroscopic factor for the (d, p) reaction as well as the systematic trend observed for several odd isotopes of tin.¹⁹

The presence of $l=1$ states at an excitation of ~ 1.9 MeV is also accounted for in a calculation by Miyake.³⁶ In this calculation states are obtained from a diagonalization of a δ plus QQ force in a quasiparticle plus zero, one and two 2^+ phonon, and zero and one 3^- phonon space. The neutron single-particle levels included were those in the 50–82 shell and the higher $2f_{7/2}$ and $3p_{3/2}$ levels. States at ~ 2 MeV with $j^\pi = \frac{3}{2}^-$ appear which have a strong component either of two 2^+ phonons coupled to an $h_{11/2}$ quasiparticle or one 2^+ phonon coupled to $f_{7/2}$ and $p_{3/2}$ quasiparticles or one 3^- phonon coupled to $d_{3/2}$ particle. The fact that the first of these configurations has the largest amplitude is a good indication that five-quasiparticle excitations are already present at these energies.

These calculations³⁶ also account for the admixtures of the collective 3^- state coupled to $s_{1/2}$ and $d_{3/2}$ quasiparticles in the wave functions of $\frac{7}{2}^-$ states at excitations near 2.6 MeV.

C. Spectroscopic-factor sums and single-particle energies

As a way of giving an over-all picture of our results we interpret them within the framework of the pairing theory.¹⁴ The sum of the spectroscopic factors for each subshell should give a measure of the nonoccupation U_{ij}^2 of that subshell in the target nucleus

$$U_{ij}^2 = \sum_{\eta} S_{ij}(\eta), \quad (1)$$

where $S_{ij}(\eta)$ is the spectroscopic factor for the state η and the sum is over all levels of the subshell. The average number of neutron holes in each subshell is then given by

$$\bar{\eta}_{ij} = (2j+1) \sum_{\eta} S_{ij}(\eta).$$

The single-quasiparticle energies E_{ij} of Kisslinger and Sorensen¹⁴ can be related to the experimental data if they are taken to be the “centers of gravity” of the observed states for a given subshell defined as

$$E'_{ij} = \frac{\sum_{\eta} E_{ij}^*(\eta) S_{ij}(\eta)}{\sum_{\eta} S_{ij}(\eta)}, \quad (2)$$

where $E_{ij}^*(\eta)$ is the excitation energy of state η . In pairing theory the nonoccupation probability U_{ij}^2 is related to the single-quasiparticle energy E_{ij} and to the single-particle energy ϵ_j of the shell model by

$$U_{ij}^2 = \frac{1}{2} [1 + (\epsilon_{ij} - \lambda)/E_{ij}] \quad (3)$$

and

$$E_{ij} = [(\epsilon_{ij} - \lambda)^2 + \Delta^2]^{1/2}, \quad (4)$$

where λ is the Fermi energy of the nucleus and Δ is one half the “energy gap.”

The spectroscopic-factor sums, the experimental centers of gravity E'_{ij} , and the average number of neutron holes are given in Table III. The position of the centers of gravity are also indicated in Fig. 6 by dashed lines. The heights of these lines are proportional to the sum of spectroscopic factors. The total number of neutron holes in the $N=50-82$ shell (and which should be contained in the first five subshells listed in Table III) should be 12 under the assumption that the next major shell is empty and the lower one is completely full. Our experimental value is 9.2, approximately 25% short of the expected value but within the limits of

TABLE III. Centers of gravity E'_{lj} , nonoccupation probabilities $U_{lj}^2 = \sum_{\eta} S_{lj}(\eta)$, and average number of neutron holes $\bar{n}_{lj} = (2j+1)U_{lj}^2$ for ^{120}Sn .

Nlj	E'_{lj} (MeV)	$\sum_{\eta} S_{lj}(\eta)$	\bar{n}_{lj}
$2d_{3/2}$	0.0	0.44	1.76
$1h_{11/2}$	0.008	0.49	5.88
$3s_{1/2}$	0.207	0.32	0.64
$1g_{7/2}$	0.994	0.04	0.32
$2d_{5/2}$	1.175	0.10	0.60
$2f_{7/2}$	>2.88	0.38	...
$3p_{3/2}$	>3.75	0.49	...

the uncertainty in the absolute values for the spectroscopic factors. A spectroscopic-factor sum of unity should be obtained for the two higher subshells listed in Table III under the above assumptions. The experimental values indicate that roughly only 50% of the $f_{7/2}$ and $p_{3/2}$ strengths have been located.

The prediction of Eqs. (3) and (4) is shown in Fig. 7. The energy 2Δ necessary to break a neutron pair was assumed to be given by the odd-even mass difference, i.e.,

$$2\Delta = 2[M(A) - \frac{1}{2}[M(A+1) - M(A-1)]] = 2.62 \text{ MeV.}$$

In Fig. 7 the position of the full curve was adjusted relative to the lowest center of gravity (the $d_{3/2}$ state) using the value of $(\epsilon_{d_{3/2}} - \lambda)$ predicted by Eqs. (2) and (3) by substituting the experimental value of the spectroscopic-factor sum in the left-hand side of Eq. (2). The remaining single-particle energies were then calculated from Eq. (3) using the known differences of energy between the experimental centers of gravity. The reasonable agreement represented by the small differences between the experimental values and the theoretical expectations in Fig. 7 should not be taken as too significant since a single nucleus is being considered here and no adjustment of parameters (e.g., ϵ_{lj} and Δ) has been attempted to obtain a best fit to data involving neighboring nuclei. The uncertainties in the spectroscopic factors also prevent more definite conclusions to be drawn and the comparison with pairing theory presented in Fig. 7 should be taken only as a useful way of presenting the experimental data.

The $h_{11/2}$ and $d_{3/2}$ single-particle states which were below the Fermi surface for the lighter isotopes^{17, 18} are now crossing it as a result of the increase in the number of neutrons. The $f_{7/2}$ and $p_{3/2}$ levels, belonging to the next major shell, are expected to lie high above the Fermi surface.

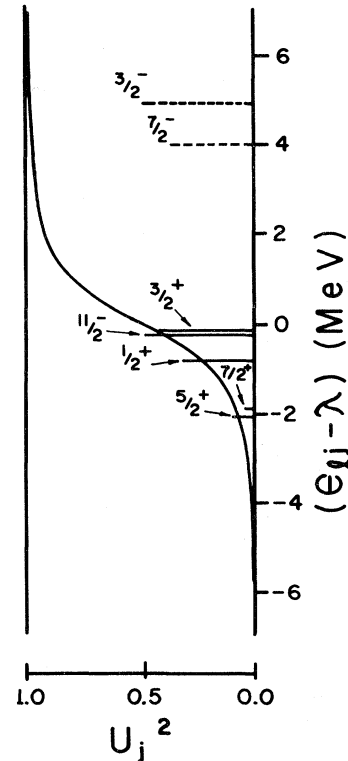


FIG. 7. Comparison of the summed spectroscopic factors (heavy horizontal lines) with the predictions from pairing theory (full curve) given by Eq. (3).

Even though the application of pairing theory is questionable in that case, we use Eq. (3) to obtain lower limits for the relative positions of the respective single-particle energies. A different interpretation of the data concerning the $l=2$ states would affect the comparison between theory and experiment since the $d_{5/2}$ single-particle level was used as a reference. The only $l=2$ state which has a questionable spin assignment is state No. 3 at 899 keV. Its spectroscopic strength is quite small however and no significant differences should be observed if this state indeed has $j^\pi = \frac{3}{2}^+$ instead of being a $d_{5/2}$ as assumed in the present work.

ACKNOWLEDGMENTS

The authors are indebted to E. W. Hamburger and B. L. Cohen for their continued support and interest in the present project. The helpful discussions with H. Miyake and A. F. T. Piza and their communication of calculations prior to publication are appreciated.

- *This work was partially supported by Fundação de Amparo à Pesquisa do Estado de São Paulo, Banco Nacional do Desenvolvimento Econômico and Conselho Nacional de Pesquisas at the University of São Paulo, and by the National Science Foundation at the University of Pittsburgh.
- †Work performed in partial fulfillment of M.Sc. degree requirements at the University of São Paulo.
- ‡Present address: Nuclear Physics Laboratory, University of Oxford, Keble Road, Oxford, England.
- ¹B. L. Cohen and R. E. Price, *Phys. Rev.* **121**, 1441 (1961).
- ²E. J. Schneid, A. Prakash, and B. L. Cohen, *Phys. Rev.* **156**, 1316 (1967).
- ³C. L. Nealy and R. K. Sheline, *Phys. Rev.* **135**, B325 (1964).
- ⁴D. L. Powell, P. J. Dallimore, and W. F. Davidson, *Aust. J. Phys.* **24**, 793 (1971).
- ⁵C. R. Bingham and D. L. Hillis, *Phys. Rev. C* **8**, 729 (1973).
- ⁶P. E. Cavanagh, C. F. Coleman, A. G. Hardacre, G. A. Gard, and J. F. Turner, *Nucl. Phys.* **A141**, 97 (1970).
- ⁷R. F. Casten, E. R. Flynn, O. Hansen, and T. J. Mulligan, *Nucl. Phys.* **A180**, 49 (1972).
- ⁸D. G. Fleming, M. Blann, and H. W. Fulbright, *Nucl. Phys.* **A163**, 401 (1971).
- ⁹R. L. Robinson, F. K. McGowan, P. H. Stelson, W. T. Milner, and R. O. Sayer, *Nucl. Phys.* **A123**, 193 (1969).
- ¹⁰P. H. Stelson, W. T. Milner, F. K. McGowan, R. L. Robinson, and S. Raman, *Nucl. Phys.* **A190**, 197 (1972).
- ¹¹Y. S. Kim and B. L. Cohen, *Phys. Rev.* **142**, 788 (1966).
- ¹²K. Yagi, Y. Saji, T. Ishimatsu, Y. Ishizaki, M. Matoba, Y. Nakajima, and C. Y. Huang, *Nucl. Phys.* **A111**, 129 (1968).
- ¹³E. U. Baranger, in *Advances in Nuclear Physics*, edited by M. Baranger and E. Vogt (Plenum, New York, 1971), Vol. 4, p. 261.
- ¹⁴L. S. Kisslinger and R. A. Sorensen, *Rev. Mod. Phys.* **35**, 853 (1963).
- ¹⁵T. T. S. Kuo, E. U. Baranger, and M. Baranger, *Nucl. Phys.* **79**, 513 (1966).
- ¹⁶R. Alzetta and J. Sawicki, *Phys. Rev.* **173**, 1185 (1968).
- ¹⁷T. Borello, E. Frota-Pessoa, C. Q. Orsini, O. Dietzsch, and E. W. Hamburger, *Rev. Bras. Fis.* **2**, 157 (1972).
- ¹⁸T. Borello-Lewin, C. Q. Orsini, O. Dietzsch, and E. W. Hamburger, unpublished.
- ¹⁹M. J. Bechara, T. Borello-Lewin, O. Dietzsch, E. W. Hamburger, H. Miyake, and A. F. T. Piza, in *Proceedings of the International Conference on Nuclear Physics, Munich, 1973*, edited by J. de Boer and H. J. Mang (North-Holland, Amsterdam/American Elsevier, New York, 1973), Vol. 1, p. 224.
- ²⁰B. L. Cohen, J. B. Moorhead, and R. A. Moyer, *Phys. Rev.* **161**, 1257 (1967).
- ²¹W. W. Daehnick, *Phys. Rev.* **177**, 1763 (1969).
- ²²J. E. Spencer and H. A. Enge, *Nucl. Instrum. Methods* **49**, 181 (1967).
- ²³J. B. Moorhead and R. A. Moyer, private communication; M. J. Bechara and O. Dietzsch, unpublished.
- ²⁴R. H. Bassel, R. M. Drisko, and G. R. Satchler, Oak Ridge National Laboratory Report No. ORNL-3240 (unpublished).
- ²⁵F. G. Perey, *Phys. Rev.* **131**, 745 (1963).
- ²⁶C. M. Perey and F. G. Perey, *Phys. Rev.* **132**, 755 (1963).
- ²⁷P. D. Kunz, University of Colorado, distorted-wave Born approximation computer code dwuck and instructions (unpublished).
- ²⁸B. L. Cohen, in *Nuclear Spin Parity Assignments*, edited by N. B. Gove (Academic, New York, 1966), p. 365.
- ²⁹D. J. Horen, *Nucl. Data* **B6**, 75 (1971).
- ³⁰R. E. Snyder and G. B. Beard, *Nucl. Phys.* **A113**, 581 (1968).
- ³¹P. Richard, C. F. Moore, J. A. Becker, and J. D. Fox, *Phys. Rev.* **145**, 971 (1966).
- ³²L. Veaser and J. Ellis, *Nucl. Phys.* **A115**, 185 (1968).
- ³³O. Dietzsch, E. W. Hamburger, and K. Schechet, *Bull. Am. Phys. Soc.* **12**, 19 (1967); M. S. Assumpção, H. Miyake, O. Dietzsch, and E. W. Hamburger, unpublished.
- ³⁴R. Arking, R. N. Boyd, J. C. Lombardi, A. B. Robbins, and B. Gonsior, *Nucl. Phys.* **A155**, 480 (1970).
- ³⁵S. de Barros, M. J. Bechara, T. Borello-Lewin, and V. Paar, *Phys. Lett.* **49B**, 113 (1974).
- ³⁶H. Miyake (private communication).